Received March 20, 2022, accepted April 6, 2022, date of publication April 22, 2022, date of current version April 29, 2022.
Digital Object Identifier 10.1109/ACCESS.2022.3169600

Stochastic Optimal Power Flow for Power Systems Considering Wind Farms Based on the Stochastic Collocation Method

BINGQING XIA, YUWEI CHEN, WENBIN YANG, (Member, IEEE), QING CHEN, (Member, IEEE), XIAOHE WANG, AND KUAN MIN
Powerchina Huadong Engineering Corporation Ltd., Hangzhou 311122, China
Corresponding author: Bingqing Xia (bqxia@zju.edu.cn)

This work was supported by the Science and Technology Project from the Powerchina Huadong Engineering Corporation Ltd., China, under Grant KY2018-XNY-02.

ABSTRACT The investigation of stochastic optimal power flow (SOPF) is to seek the optimal solution of static stability constrained optimal power flow considering the uncertainty of parameters in power systems. To solve the problem, this paper proposes an approach based on the stochastic collocation method (SCM) and Gram-Charlier expansion to obtain the optimal solution of SOPF. Firstly, the SOPF model to simultaneously consider uncertainties and static stability is formulated. Then, probabilistic chance constraints are reformulated as a set of deterministic constraints using polynomial approximation, which explicitly describe the relationship between the probability of chance constraints and control variables. By applying the primal-dual interior point method to the reformulated SOPF model, the optimal solution can be efficiently obtained. The proposed SCM-based approach has been thoroughly tested on a modified 3-machine 9-bus system and IEEE 118-bus system, which verifies the effectiveness and accuracy of the proposed method.

INDEX TERMS Stochastic optimal power flow, wind farms, uncertain parameters, stochastic collocation method, Gram-Charlier expansion.

I. INTRODUCTION

The optimal power flow (OPF) problem [1], [2] is one of the most important tools for power system planning and operation. Since the modern interior point method has been applied to power system optimization calculation [3]–[6], the solution of OPF problems for large-scale power systems has been successfully realized. The traditional OPF problem is based on a deterministic model, which ignores the stochastic factors in the system. However, due to the errors in the process of power system state measurement and data transmission, the system load level and network state are not deterministic quantities. In addition, in recent years, in order to realize the cleanliness of the power side of the smart grid, large-scale renewable energy (such as wind power, solar power, etc.) is connected to the power system in the form of centralized or distributed power generation, and the power output of these renewable energy plants is strongly random and intermittent with the influence of natural conditions (such as wind speed, light intensity and time, etc.), which makes the solution of the OPF problem need to face more uncertain factors.

Generally, the OPF problem under uncertainty is formulated as an nonlinear algebraic programming (NLP). There are three main methods to consider the uncertain parameters in OPF: 1) the robust OPF [7]–[13], which makes the system robust stable to the random variations of parameters. It only requires knowledge of the variation range of uncertain parameters, and is therefore more computationally efficient. However, since it ignores the statistic characteristics of uncertain parameters, it usually results in the worst-case scenario and conservative solutions; 2)the probabilistic OPF (POPF) [14]–[19], which is a stochastic analysis problem in which information on the probability distribution of several

The associate editor coordinating the review of this manuscript and approving it for publication was Shiwei Xia.

state variables (such as the objective function of the OPF, the output of each generator, the output of the reactive power source, the bus voltage amplitude, etc.) is obtained based on the probability distribution of known random variables. 3) the stochastic OPF (SOPF), which limits the probability of constraints' violation affected by uncertain parameters to an assigned value. Many methods have been proposed to solve the SOPF, for example, in reference [20], the Benders decomposition was used to solve the security-constrained unit commitment problem considering the intermittency wind power generation, where possible scenarios are simulated for representing the wind power volatility. In reference [21], random disturbances are modeled as scenario trees using the Monte Carlo simulation method and the optimization problem is decomposed into deterministic long term security-constrained unit commitment subproblems. In reference [22], [23], the problem is formulated as a chance-constrained two-stage stochastic program and algorithms are developed to solve the model effectively. The POPF and SOPF rely on a presumed probability density function (PDF) of uncertain parameters, and they usually need a huge number of sampling scenarios. The difficulty in solving SOPF lies in the treatment of chance constraints. Generally, heuristic optimization methods or transformation of the stochastic optimization model into a deterministic optimization model can be used to solve the problem, which requiring repeated iterative solutions. To avoid this, we propose a stochastic Collocation method (SCM)-based approach to solve SOPF in this paper, which aims to transform the stochastic optimization model into a deterministic optimization model under the premise of fewer samplings. The advantage of the proposed method is that the obtained polynomial approximation can avoid large random sampling of the power system, thus it can improve the computational efficiency of the optimal solution while ensuring the reliability of the optimal solution.

To reformulate the SOPF model, the effect of uncertain parameters and control variables on static stability needs to be thoroughly quantified at first. The Monte Carlo method [25] is a straightforward method adopted to estimate the statistical characteristic of the static states according to the probability distribution of uncertain parameters, which requires a large number of sample data and repeated dynamic simulation, thus this method can become time-consuming.

To improve computation efficiency, polynomial chaos expansion (PCE) methods have been widely researched in probabilistic studies [26], [27], and has been applied to all kinds of static or dynamic problems in many engineering fields, e.g. electrical power systems [28]–[31], electric circuits [32], fluid dynamics [33] and control engineering [34]. PCE methods are based on the polynomial approximation theory, i.e., use a linear combination of a set of polynomial basis functions with undetermined coefficients to approximate the relationship between the desired system outputs and uncertain parameters explicitly (called polynomial approximation), and then calculate the probability distributions of system outputs by this polynomial approximation.

The SCM [26]–[28] is an effective way to solve undetermined coefficients in PCE. It is a non-intrusive PCE method that treats the system model as a black box and only needs to acquire values of parameter-output function at the collocation points from the system model. Therefore, the SCM's solvability only relies on the solvability of the existing system program, and has nothing to do with the system size and parameter number. Inspired by this, in this paper, we adopt the SCM method to analyze the static stability by constructing the polynomial approximation of static states concerning parameters.

Since static states have been approximated by polynomials, the moments of static states can be easily obtained. Then, by the SCM and the Gram-Charlier expansion, the relationship between the control variables and the probability of chance constraints can be expressed by a set of polynomials. Therefore, the initial probabilistic algebraic NLP of SOPF can be reformulated as a deterministic algebraic NLP. By applying the classic primal-dual interior point method (PDIPM) [5] to the reformulated SOPF model, the optimal solution can be efficiently obtained. In this paper, the proposed approach is thoroughly tested and evaluated using the 3-machine 9-bus system and the IEEE 118-bus system.

The main contributions of this paper include: 1) the proposed SCM-based approach can efficiently solve the SOPF problem, which can obtain optimal control scheme without large amount of sampling; 2) the proposed SCM-based approach can construct the quantitive relationship between the static states and random parameters, through which the effect of uncertain parameters on the static stability can be analyzed. 3) the proposed method for SOPF problem is general and flexible to be cooperated with existing system programs, and its solvability will not be limited by system size and parameter number.

The rest of this paper is organized as follows. The model of the SOPF problem is first introduced in Section II. In Section III, the SCM-based algorithm is formed to reformulate the SOPF model and solve the OPF problem. Section IV summerizes the procedures of the proposed method and Section V validates this method on the 3-machine 9-bus system and IEEE 118-bus system. Conclusions and future work are given in the last Section.

II. FORMULATION OF PROBABILISTIC TRANSIENT STABILITY CONSTRAINED OPTIMAL POWER FLOW

A. GENERAL MATHEMATICAL MODEL OF SOPF

Aiming to adjust control variables to make the system stable with a satisfactory security level, the SOPF is formulated as the following algebraic NLP problem:

$$\min E\{c(\mathbf{y}, \mathbf{u}, \mathbf{p})\} \tag{1}$$

Subject to :

$$\mathbf{0} = \mathbf{g}(\mathbf{y}, \mathbf{u}, \mathbf{p}) \tag{2}$$

$$P\{\mathbf{H}(\mathbf{y},\mathbf{u},\mathbf{p}) \leq \mathbf{H}_{\max}\} \geq \boldsymbol{\beta} \tag{3}$$

where $\mathbf{y} \in \mathbf{R}^{n_y}$ denotes the algebraic variables such as the bus voltage and injection current; $\mathbf{u} \in \mathbf{R}^{n_u}$ denotes the control variables with lower and upper limits, such as the generator active power and terminal voltage; $\mathbf{p} = (p_1, \ldots, p_{n_p}) \in \mathbf{D} = (D_1, \ldots, D_{n_p})$ denotes the uncertain parameters, such as nodal load and the injected power by energy sources. $E\{*\}$ in (2) stands for the expectation calculation, and the objective function $c : \mathbf{R}^{n_y} \times \mathbf{R}^{n_u} \times \mathbf{R}^{n_p} \rightarrow R$ can be expressed as the fuel cost, network loss, or the interface transfer capability etc.. $\mathbf{g} : \mathbf{R}^{n_y} \times \mathbf{R}^{n_u} \times \mathbf{R}^{n_p} \rightarrow \mathbf{R}^{n_y}$ is the vector of functions corresponding to the algebraic part of power system model, which included the models of network and energy sources. (2) is the steady-state equality constraints including power flow balances, which are the steady-state equality constraints. $P\{*\}$ in (3) stands for the probability calculation, and (3) requires the chance constraints for steady-state variables above a fixed risk security level β_0, which includes limits on bus voltage magnitude, generator active and reactive power outputs, etc.

B. EXPLICIT FORMULATION OF SOPF PROBLEM CONSIDERING WIND GENERATION

While the general form of SOPF model is presented in Section II-A, here a representative SOPF model used in the case study is explicitly given with brief descriptions on how various uncertain variables could be considered in SOPF. In this paper, only load injections and wind generations are considered in the SOPF problem, while other common uncertain factors could be easily tackled in a similar way.

1) OBJECTIVE FUNCTION

Usually, slack bus generator is used to keep the power balance in the system. However, the uncertainties of random input variables would cause the slack bus generation become probabilistic. Therefore, the system state variables and concerned objectives will be probabilistic too. In this paper, the expected total generation fuel cost [24] is adopted as the objective of the SOPF model

$$E\{\sum_{i=1}^{n_G}(a_i P_{Gi}^2 + b_i P_{Gi} + c_i)\} \tag{4}$$

where $E\{\cdot\}$ is the is the expectation calculation operator, P_{Gi} is active power of the ith generator, a_i, b_i and c_i are the fuel coefficients corresponding to the different order terms of generator i respectively and n_G is total number of traditional generators. It shall be noted that there is no limitation on the formulation of the SOPF objective, and many other targets, such as expected minimum power loss, expected participants' bids in power market, could be similarly designed as the objective of SOPF or even extended to form a multiple-objective SOPF model.

2) STATIC EQUALITY CONSTRAINTS

The static equality constraint (2) is explicitly described by the power flow equations as

$$\begin{cases} 0 = P_{Gi} + P_w - P_{Di} - V_i \sum_{j=1}^{n_b} V_j (G_{ij}\cos\theta_{ij} + B_{ij}\sin\theta_{ij}) \\ 0 = Q_{Gi} + Q_w - Q_{Di} - V_i \sum_{j=1}^{n_b} V_j (G_{ij}\sin\theta_{ij} - B_{ij}\cos\theta_{ij}) \end{cases} \tag{5}$$

where $i = 1, 2, \ldots, n_b$, n_b is the total number of buses; Q_{Gi} and Q_{Di} are the generator and load reactive power, V_i and V_j are the voltage magnitude of bus i and j, θ_{ij} is the angle difference between bus i and j.

3) STATIC PROBABILISTIC INEQUALITY CONSTRAINTS

The static inequality constraint (3) explicitly includes the probabilistic constraints for generator reactive power, node voltage and transmission line thermal limits as

$$P\{Q_{Gi\min} \leq Q_{Gi} \leq Q_{Gi\max}\} > \beta_Q (i = 1, 2, \ldots, n_G) \tag{6}$$

$$P\{V_{i\min} \leq V_i \leq V_{i\max}\} > \beta_V (i = 1, 2, \ldots, n_b) \tag{7}$$

$$P\{S_{li} \leq S_{li\max}\} > \beta_S (i = 1, 2, \ldots, n_l) \tag{8}$$

where n_l is the number of branches and S_{li} is the apparent power flow in the ith branch; $Q_{Gi\min}$, $Q_{Gi\max}$, $V_{Gi\min}$ and $V_{Gi\max}$ are the lower and upper limits of generator reactive power and bus voltage, respectively; $S_{li.max}$ is upper limit of the ith transmission line power. These probabilistic constraints ensure that bus voltages, generator reactive power and transmission line power flows are all bounded in the required ranges with an acceptable risk security level.

4) WIND GENERATIONS

With variable wind speed, a wind generator output is determined from the speed-power curve of wind turbine,

$$P_w = \begin{cases} 0, & (v_w < v_{ci}, v_w > v_{ct}) \\ P_{rated}(\frac{v_w - v_{ci}}{v_{rd} - v_{ci}}), & (v_{ci} \leq v_w \leq v_{rd}) \\ P_{rated}, & (v_{rd} < v_w < v_{ct}) \end{cases} \tag{9}$$

where P_{rated} is the rated power, v_{ci}, v_{rd} and v_{ct} are the cut-in, rated and cut-out wind speed, respectively. The distribution of wind generations can be calculated from (9) using the wind speed samples based on its probabilistic model.

III. METHODOLOGY

A. POLYNOMIAL APPROXIMATION OF STATIC STATES

Since both control variables $\mathbf{u}$ and uncertain parameters $\mathbf{p}$ have effect on the static system variables $\mathbf{y}$, they are analyzed together for simplification in this section. We will use $\mathbf{p}' = [\mathbf{u}^T, \mathbf{p}^T]^T$ as a compact form of control variables $\mathbf{u}$ and uncertain parameters $\mathbf{p}$.

As can be seen from the static equality constraints (2), the relationship between $\mathbf{p}'$ and desired system outputs $\mathbf{y}$ is implicitly described by a set of algebraic equations. In order to investigate the effect of parameters $\mathbf{p}$ on static stability, the SCM is introduced to approximate the relationship between the static system outputs $\mathbf{y}$ and uncertain parameters $\mathbf{p}'$ explicitly with polynomial expression.

Firstly, assume $|\partial\mathbf{g}/\partial\mathbf{y}| \neq \mathbf{0}$, then according to the implicit function theorem, static constraints (2) can be solved locally by:

$$\mathbf{y}(\mathbf{p}') \approx \hat{\mathbf{y}}(\mathbf{p}') = \sum_{k=1}^{N_\mathrm{b}} \mathbf{c}_k^{\mathbf{y}} \Phi_k(\mathbf{p}'), \tag{10}$$

where $\mathbf{c}_k^{\mathbf{y}}$ is the vector of undetermined coefficients which are time varied; $\Phi_k(\mathbf{p}')$ is the k-th orthogonal polynomial basis function of multiple parameters, which is $\Phi_k(\mathbf{p}') \triangleq \left\{\varphi_{k_1}(p_1')\varphi_{k_2}(p_2')\cdots\varphi_{k_d}(p_d')\right\}$. Here $\varphi_{k_d}(p_d')$ is the orthogonal polynomial basis function in d-th dimension of $\mathbf{p}'$, $k_i, i = 1, 2, \ldots, d$ is the order of i-th dimensional polynomial basis function, and the sort order of the subscript k satisfies: $k < j$, if $\bigwedge_{i=1}^{d}(k_i < j_i)$. $N_\mathrm{b} = \dfrac{(N+d)!}{N!d!}$ is the number of polynomial basis functions, i.e. undetermined coefficients, where N is the total degree of the polynomial basis functions $\left\{\Phi(\mathbf{p}')\right\}$ and $d = n_\mathrm{u} + n_\mathrm{p}$ is the dimension of parameters $\mathbf{p}'$. Note that the choice of unidimensional orthogonal polynomial basis function $\varphi_{k_d}(p_d')$ depends on the distribution of p_d'. This selection method is called the Askey scheme [27], which provides some typical probability distribution and corresponding orthogonal polynomials.

Then, the undetermined coefficients $\mathbf{c}_k^{\mathbf{y}}$ in (10) can be solved by the SCM with the following formula:

$$\mathbf{c}_k^{\mathbf{y}} = \frac{1}{\chi_k}\sum_{m=1}^{M} \alpha_m \Phi_k(\mathbf{p}'^{(m)})\mathbf{y}(\mathbf{p}'^{(m)}), \tag{11}$$

where $\chi_k = \int_{D'} \Phi_k(\mathbf{p}')\Phi_k(\mathbf{p}')\omega(\mathbf{p}')\mathrm{d}\mathbf{p}'$, and D' is the domain of $\mathbf{p}'$; $\mathbf{p}'^{(m)}$, $m = 1, \ldots, M$ are collocation points (also called integration points), and α_m is the integration coefficient of $\mathbf{p}'^{(m)}$. The collocation points and corresponding integration coefficient α_m are determined through the Smolyak sparse grid quadrature [26]; $\mathbf{y}(\mathbf{p}'^{(m)})$ is the value of $\mathbf{y}$ with $\mathbf{p}' = \mathbf{p}'^{(m)}$, which can be obtained through solving (5). For the proposed method, the sampling points are the tensor products of the Gaussian integration points required for each one-dimensional parameter. Therefore, the sampling points required by the proposed method are not randomly generated, but are determined by both the dimensionality of the parameters and the order of the polynomial approximation. When the data of the required sampling points are insufficient, it will lead to the loss of accuracy in the calculation of the approximation coefficients by Eq. (11), which in turn will lead to the loss of reliability of the solution of the SOPF.

With the polynomial formulation, the i^{th} moments of the static variables can be readily approximated by applying their definitions directly to the polynomial approximation (10), such as

$$\mu_i^{\mathbf{y}} \triangleq E\{\hat{\mathbf{y}^i}(\mathbf{p}')\} = \int \hat{\mathbf{y}}^i(\mathbf{p}')\omega(\mathbf{p})\mathrm{d}\mathbf{p}, \tag{12}$$

where $\omega(\mathbf{p})$ is the probability density function (PDF) of the uncertain parameter. With these moments, the CDF of static/transient variables derived using methods such as the Gram-Charlier (GC) expansion [24].

B. REFORMULATION OF SOPF MODEL

In last subsection, the polynomial expansion of all static variables has been obtained using the SCM. Therefore, all variables in the SOPF model can be substituted by their polynomial expansions. In this section, we will present how to use polynomial expansions to transform the original probabilistic NLP problem into a deterministic NLP problem.

1) REFORMULATION OF OBJECTIVE FUNCTION

As for the objective function $E\{c(\mathbf{y}, \mathbf{u}, \mathbf{p})\}$, when we substitute $\mathbf{y}$ with their polynomial expansions, the expectation considering the uncertain parameters can be derived by

$$\begin{aligned} E\{c(\mathbf{y}, \mathbf{u}, \mathbf{p})\} &\approx \int c(\sum_{k=1}^{N_\mathrm{b}} \mathbf{c}_k^{\mathbf{y}} \Phi_k(\mathbf{u}, \mathbf{p})\omega(\mathbf{p})d\mathbf{p} \\ &= c'(\mathbf{u}). \end{aligned} \tag{13}$$

Therefore, the reformulated objective function is a function in terms of control variables $\mathbf{u}$.

2) REFORMULATION OF PROBABILISTIC STATIC STABILITY CONSTRAINTS

In order to evaluate the the probabilistic static stablity constraints, probability $P\{\mathbf{H}(\mathbf{y}, \mathbf{u}, \mathbf{p}) \leq \mathbf{H}_{\max}\}$ need to be evaluate first. Note that both uncertain parameter $\mathbf{p}$ and control variables $\mathbf{u}$ are included in variables' polynomial expansions, but only the uncertainty of $\mathbf{p}$ need to be quantified. Therefore, $P\{\mathbf{H}(\mathbf{y}, \mathbf{u}, \mathbf{p}) \leq \mathbf{H}_{\max}\}$ are functions in terms of control variables. In this subsection, an approach based on the SCM and the Gram-Charlier expansion is proposed to approximate these functions and reformulate the probabilistic static/transient stability constraints.

The main procedures are presented as follows:

1) Give the set of collocation points of control variables according to the Smolyak sparse grid quadrature as $\mathbf{u}^{(m)}, m = 1, \ldots, M$.
2) For each $\mathbf{u}^{(m)}$, evaluate the probability of $\mathbf{H}(\mathbf{y}, \mathbf{u}, \mathbf{p}) \leq \mathbf{H}_{\max}$ using the Gram-Charlier expansion by

$$\begin{aligned} &P\{\mathbf{H}(\mathbf{y}, \mathbf{u}, \mathbf{p}) \leq \mathbf{H}_{\max}\}|_{\mathbf{u}^{(m)}} \\ &\quad = \int_{-\infty}^{\tilde{\mathbf{H}}_{\max}} N(u)du - N(\tilde{\mathbf{H}}_{\max})[\frac{K_3}{3!\sigma^3}(\tilde{\mathbf{H}}_{\max}^2 - 1) \\ &\qquad + \frac{K_4}{4!\sigma^4}(\tilde{\mathbf{H}}_{\max}^3 - 3\tilde{\mathbf{H}}_{\max}) \\ &\qquad + \frac{K_5}{5!\sigma^5}(\tilde{\mathbf{H}}_{\max}^4 - 6\tilde{\mathbf{H}}_{\max}^2 + 3)], \end{aligned} \tag{14}$$

where $\tilde{\mathbf{H}}_{\max} = (\mathbf{H}_{\max} - \mu)/\sigma$, μ and σ are the mean value and the standard deviation of $\mathbf{H}(\mathbf{y}, \mathbf{u}^{(m)}, \mathbf{p})$; $N(*)$ is the standard normal distribution function; K_j are the

j^{th} cumulants of $\mathbf{H}(\mathbf{y}, \mathbf{u}^{(m)}, \mathbf{p})$ which can be derived from the moments of $\mathbf{H}(\mathbf{y}, \mathbf{u}^{(m)}, \mathbf{p})$.

3) Based on the SCM, the polynomial expansion of probability $P\{\mathbf{H}(\mathbf{y}, \mathbf{u}, \mathbf{p}) \leq \mathbf{H}_{\max}\}$ can be constructed by

$$P\{\mathbf{H}(\mathbf{y}, \mathbf{u}, \mathbf{p}) \leq \mathbf{H}_{\max}\}|_{\mathbf{u}} \approx \hat{P}\{\mathbf{H}(\mathbf{y}, \mathbf{u}, \mathbf{p}) \leq \mathbf{H}_{\max}\}|_{\mathbf{u}} = \sum_{k=1}^{N_b} \mathbf{c}_k^P \Phi_k(\mathbf{u}), \tag{15}$$

with

$$\mathbf{c}_k^P = \frac{1}{\chi_k} \sum_{m=1}^{M} \alpha_m \Phi_k(\mathbf{u}^{(m)}) P\{\mathbf{H}(\mathbf{y}, \mathbf{u}, \mathbf{p}) \leq \mathbf{H}_{\max}\}|_{\mathbf{u}^{(m)}} \tag{16}$$

4) Static stability constraints (3) can be reformulated as

$$P\{\mathbf{H}(\mathbf{y}, \mathbf{u}, \mathbf{p}) \leq \mathbf{H}_{\max}\}|_{\mathbf{u}} \approx \sum_{k=1}^{N_b} \mathbf{c}_k^P \Phi_k(\mathbf{u}) \geq \boldsymbol{\beta} \tag{17}$$

So far, uncertain parameters have been eliminated from the model of SOPF, and the following algebraic NLP is formulated:

$$\min \ c'(\mathbf{u}) \tag{18}$$

Subject to static stability constraints:

$$\sum_{k=1}^{N_b} \mathbf{c}_k^{P\{\mathbf{H} \leq \mathbf{H}_{\max}\}} \Phi_k(\mathbf{u}) \geq \boldsymbol{\beta} \tag{19}$$

When constraint (19) is included in the SOPF formulation, the static constrains (2) are also included implicitly. Therefore these constraints and the corresponding variables $\mathbf{y}$ can be eliminated from the formulation of SOPF. The reformulation of SOPF model gives the following advantages:

1) The chance constraint (3) in the general SOPF can not be dealt with directly by existing optimization methods. Differently, the reformulated SOPF model is deterministic, which can be easily dealt with.
2) The dimension of the optimization model is largely reduced. With the elimination of the static constrains (2), the dimension of the optimization model are less than that of a conventional OPF.
3) The uncertainty of parameters $\mathbf{p}$ in the SOPF model has been thoroughly quantified, the optimal solution of the SOPF can be directly obtained through solving the reformulated SOPF model (18)-(19) without any iteration.

C. PDIMP FOR SOLVING THE REFORMUALTED SOPF

Based on the classical PDIPM [5], by introducing slack variables for inequality constraints (19) and appending the logarithmic barrier functions to the objective, SOPF model (18)-(19) can be reformulated as the following subproblem:

$$\min \ c'(\mathbf{u}) - \boldsymbol{\mu} \sum_{j=1}^{r} \log(\boldsymbol{\upsilon}) \tag{20}$$

Subject to :

$$\sum_{k=1}^{N_b} \mathbf{c}_k^{P\{\mathbf{H} \leq \mathbf{H}_{\max}\}} \Phi_k(\mathbf{u}) - \boldsymbol{\upsilon} = \boldsymbol{\beta} \tag{21}$$

where $\boldsymbol{\mu} > 0$ is the barrier parameter that is enforced to decrease towards zero iteratively; $\boldsymbol{\upsilon} = [\upsilon_1(\mathbf{p}), \ldots, \upsilon_r(\mathbf{p})]$ is the vector of slack variables for inequality constraints, and r is the number of static stability inequality constraints (19). As $\boldsymbol{\mu}$ tends towards zero, the solution of the reformulated subproblem approaches the solution of the primary optimization model (18)-(19). By solving the subproblem (21)-(21), the optimal solution of the reformulated SOPF problem (18)-(19) can be obtained.

IV. PROCEDURES

The main procedures of the proposed method for solving the SOPF problem are summarized below.

Step 1: Input system data and construct the parametric SOPF model, determine the uncertain parameters and controllable parameters to be considered in the stability analysis.

Step 2: In order to eliminate the power flow equation from the SOPF model, construct the polynomial approximation of static variables as Eq. (10), and then the static stability constraint in SOPF model can be reformulted as Eq. (19).

Step 3: Reformulate the SOPF model as an algebraic NLP in Eq. (18)-(19), introduce slack variables for inequality constraints (19) and appending the logarithmic barrier functions to the objective. By solving Eq. (21)-(21), the optimal control scheme of the reformulated SOPF problem can be obtained.

V. CASE STUDIES

The modified 3-machine 9-bus system with 2 wind farms as shown in Fig. 1 and IEEE 118-bus system are presented in this section. The purpose is to illustrate the characteristics and effectiveness of the proposed method through the 3-machine 9-bus system case, and to illustrate the potential of the method for practical power system applications through the IEEE 118-bus system case.

The Monte Carlo method (MCM) is conducted for benchmarking the performance of the proposed method in static stability analysis. All computations are performed on Wolfram Mathematica 12.0 on a desktop with a CPU of Intel i7-8700U 3.20 GHz and a RAM of 8:0 GB.

A. THE 3-MACHINE 9-BUS SYSTEM CASE

1) CASE SETTINGS

The detailed data of the 3-machine 9-bus system shown in Fig. 1 can be found in [29]. The slack generator is at bus 1. The controllable parameters are power generation $P_{G2} \in [60, 175]$ MW, $P_{G3} \in [40, 180]$ MW. The fuel cost coefficient for the generators is $[3, 1, 1]^T$. For wind farms at bus 6 and bus 8, an aggregated model with a

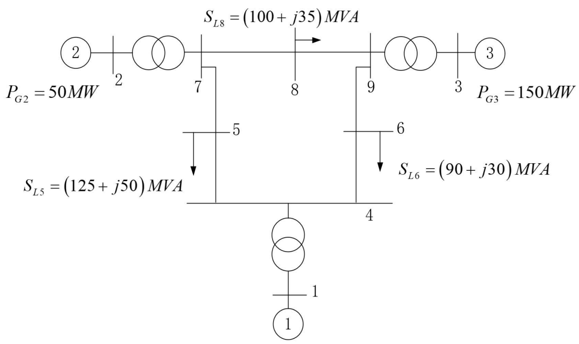

FIGURE 1. **Diagram of 9-buses system.**

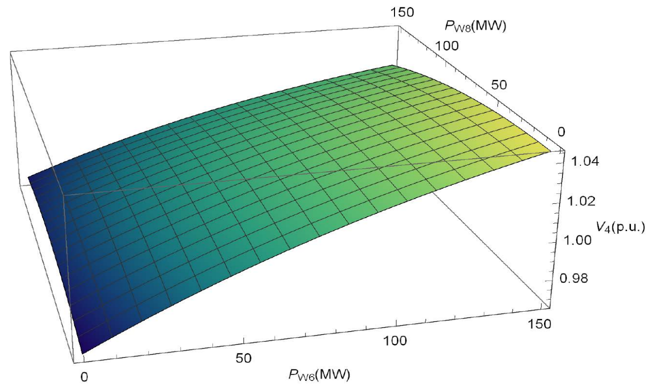

FIGURE 2. **The variation of bus voltage V_4 with uncertain parameters $P_{W6} \subseteq [0, 150]MW$ and $P_{W8} \subseteq [0, 150]MW$.**

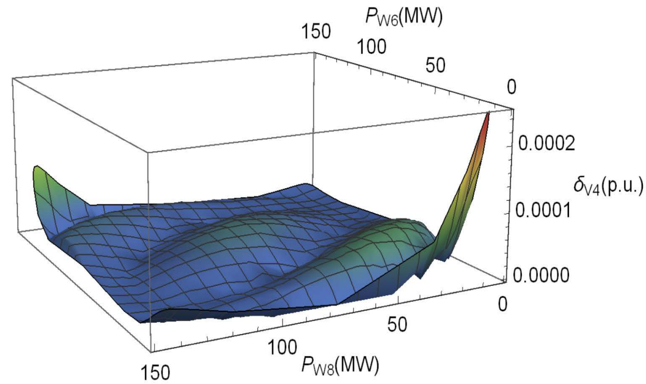

FIGURE 3. **Approximation error of the stochastic collocation method for approximating bus voltage V_4 in the 3-machine 9-bus system case.**

total number of 100 DFIGs with rated power 1.5 MW each cited from [24] are aggregated to form a wind farm respectively. Therefore, the uncertain parameter in this case is the active output of wind farms P_{W6} and P_{W8}, which varies in the range $[0, 150]$ MW. In order to keep the power factor of the wind farm constant at 0.5, the reactive power output of the wind farm will vary with the active power output.

2) APPROXIMATION ERROR AND COMPUTATION TIME OF THE PROPOSED METHOD

In order to verify the accuracy of the proposed polynomial approximation method in approximating the steady-state states, the control parameters are set to nominal values and the uncertain parameters are freely varied within their ranges. Fig. 2 plots the variation of bus voltage V_4 with the uncertain parameters P_{W6} and P_{W8}. It can be seen that V_4 increases with P_{W6}, which is due to the fact that the more power is emitted from the wind farm, the more the load power at bus 6 can be balanced locally as much as possible without the need for power generation at bus 1. As P_{W8} increases, the power flowing from bus 4 to bus 6 becomes smaller and smaller until its direction is found to change. After the change in power flow direction, the excess power from wind farms needs to be absorbed by the balancing machine at bus 1 and the voltage at bus 4 will then be reduced to accommodate the shift of power flow. Note that in the model of the SOPF, the outputs of the wind turbines are stochastic parameters and the outputs of the generators are control parameters. The aim of the SOPF is to find a set of optimal control parameters such that the probability of violating the safety constraint under the influence of the stochastic parameters is lower than a specified value. Therefore, the relationship between them is not a quantitative function relationship, it is not possible to use an image like Fig. 2 to portray the relationship between them.

To quantitatively evaluate the approximation error of the proposed SCM, we use the following absolute error $\delta_y(\mathbf{p})$ as the error index:

$$\delta_y(\mathbf{p}) \triangleq |y(\mathbf{p}) - \hat{y}(\mathbf{p})|, \tag{22}$$

where $y(\mathbf{p})$ is the actual value of y with parameter p, $\hat{y}(\mathbf{p})$ is the approximated value.

Fig. 3 plots the approximation error of voltage at bus 4. As can be seen from the figure, the approximation error of the proposed method is very small in the whole range of uncertain parameters. Moreover, the maximum approximation error does not exceed 0.00025 p.u. in this case, which shows the effectiveness of the proposed method for approximating the static states of the power system.

In the proposed method, it is necessary to first construct a polynomial approximation of the system operating state with respect to the stochastic parameters, then quantify the uncertainty of the stochastic parameters using the Gram-Charlier expansion, and finally find the optimal control scheme using the interior point method. Therefore, in order to improve the accuracy of the optimal solution, the key point is to improve the accuracy of the polynomial approximation. Based on this, the accuracy of the polynomial approximation can be improved by increasing the order of the polynomial approximation. The results in Table 1 verify that when the order of polynomial approximation is increased, the approximation error becomes smaller. The computation time of SCM with $N-th$ order of polynomial bases is also shown in Table 1. As we can see, the computation time increases

TABLE 1. Computation time and error of the polynomial approximation of static states based on the SCM in the 3-machine 9-bus system case.

Method	$\bar{\delta}_{V4}$ [1]	$\bar{\delta}_{V5}$ [1]	$\bar{\delta}_{V6}$ [1]	N_p [2]	Total time
MCM	–	–	–	500	48s
SCM(1)[3]	2.92×10^{-3}	3.12×10^{-3}	3.87×10^{-3}	5	0.5s
SCM(2)[3]	1.70×10^{-4}	1.57×10^{-4}	2.43×10^{-4}	13	1.266s
SCM(3)[3]	2.53×10^{-5}	2.45×10^{-5}	3.44×10^{-5}	29	2.844s
SCM(4)[3]	5.14×10^{-6}	4.84×10^{-6}	6.16×10^{-6}	53	5.499s
SCM(5)[3]	1.85×10^{-6}	1.74×10^{-6}	1.84×10^{-6}	89	8.828s

[1] $\bar{\delta}_{V4}$, $\bar{\delta}_{V5}$, $\bar{\delta}_{V6}$ are mean values of δ_{V4}, δ_{V5}, δ_{V6}
[2] N_p is the number of sampling points as for the MCM or the number of collocation points as for the SCM
[3] SCM(1), SCM(2), SCM(3), SCM(4), SCM(5) are SCM with 1st, 2nd, 3rd, 4th, 5th polynomial bases

rapidly with N. The reason is that the SCM need to use the simulation results at the collocation points, thus more collocation points result in more computation time. As shown in Table 1, the number of collocation points N_p increases with N, so the computation time increases with N as well. Moreover, the results in table 1 show that the approximation error becomes smaller as the order of the polynomial basis function increases. However, the approximation error is small enough at $N = 3$, and the error decreases more and more slowly with the increase of order. Therefore, considering the accuracy of approximation and computational efficiency, we set the order of polynomial approximation to $N = 3$ in this paper.

3) THE REFORMULATION OF CHANCE CONSTRAINTS

In this subsection, chance constraint $P\{S_{l4}(\mathbf{u}; \mathbf{p}) \leq S_{l4.\max}\} \geq \beta$ is used as an example to verify the effectiveness of the proposed method for chance constraint reformulation, where S_{l4} is the power flow in line 9-6, $\mathbf{u} = [P_{G2}, P_{G3}]^T$ is the vector of control parameters, $\mathbf{p} = [P_{W6}, P_{W8}]^T$ is the vector of uncertain parameters. Through the procedures of the chance constraint reformulation proposed in subsection III-B, in this case, the above chance constraint can be reconstructed as the following deterministic constraint containing only the control parameters:

$$0.231155 + 6.5 \times 10^{-3} P_{G2} - 1 \times 10^{-5} P_{G2}^2 + 0.012 P_{G3} - 4.6 \times 10^{-5} P_{G2} P_{G3} - 4.3 \times 10^{-5} P_{G3}^2 \geq \beta, \quad (23)$$

Fig. 4 plots how the left side of Eq. (23), i.e., the probability of the line power flow within its limit varies with respect to the control parameters. As we can see, probability $P\{S_{l4} \leq S_{l4.\max}\}$ will decrease as P_{G2} and P_{G3} increase. This is because line 9-6 are mainly responsible for delivering power to the load at node 6, so when the increase in P_{G2} and P_{G3} will result in more power being delivered to bus 6, which leads to a decrease in the probability of the line power flow being within the limit. Fig. 5 plots the approximation error of probability $P\{S_{l4} \leq S_{l4.\max}\}$. As can be seen from the figure, the maximum approximation error in the whole range of uncertain parameters does not exceed 0.00024, which shows

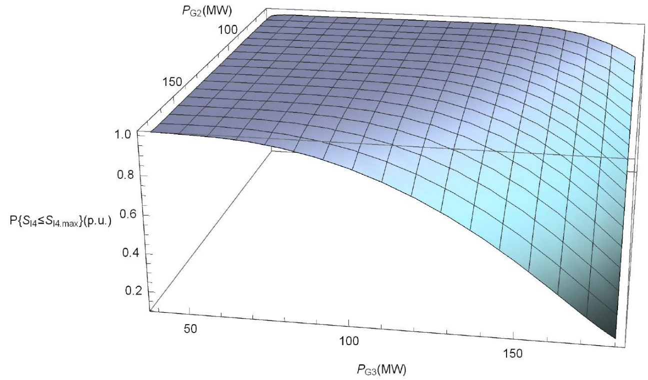

FIGURE 4. Probability of $P\{S_{l4} \leq S_{l4.\max}\}$ varies with respect to control parameters P_{G2} and P_{G3}.

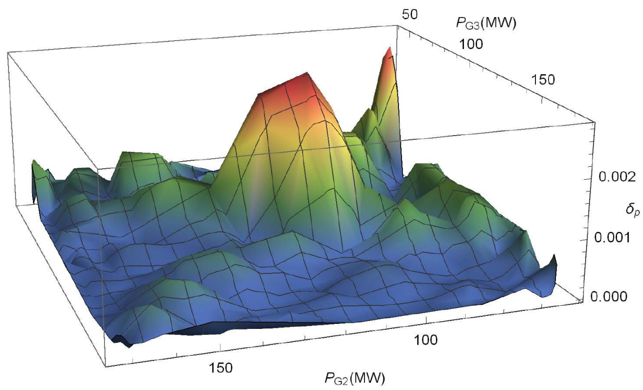

FIGURE 5. Approximation error of probability $P\{S_{l4} \leq S_{l4.\max}\}$ obtained by the proposed SCM.

TABLE 2. Optimization results of the OPF and the proposed SOPF in the 3-machine 9-bus system case.

Method	$P_{G2}(MW)$	$P_{G3}(MW)$	Cost	N[1]	Total time
OPF	130.5	156	15.654	62	0.593s
SOPF	155.4	112.1	16.6836	97	0.062s

[1] N is the number of times the line power flow S_{l4} satisfies its limit in 100 power flow calculations

the effectiveness of the proposed method for reformulation the chance constraints.

4) THE SOLUTION OF THE REFORMULATED SOPF

Table 2 gives a comparison of the optimization results of the OPF without considering the randomness of wind farms and the SOPF considering the randomness of wind farms based on the proposed SCM. The OPF is implemented with uncertain parameters $P_{W6} = P_{W8} = 120MW$. It can be seen that the fuel cost of the control scheme obtained by the SOPF is higher than that of the control scheme obtained by the OPF. However, the number of times that the line power flow satisfies its constraint when subjected to wind farm output uncertainty is 97 when the power flow calculation is run 100 times randomly, which is much higher than the 35 times when the OPF is used. In terms of computational time, the SOPF model has a higher computational efficiency in the optimization calculation because the number of constraints is smaller than the OPF model due to the elimination of the system's power flow equation in the SOPF model.

B. THE IEEE 118-BUS SYSTEM CASE

The detailed data of the IEEE 118-bus system can be found in [35]. In this case, two wind farms are added at bus 59 and bus 80 to verify the effectiveness of the proposed method. The variation range of the uncertain wind power generation P_{W59}, P_{W80} is [0, 154.5] MW and [0, 477] MW respectively, and each wind farm consists of DFIGs with rated power 1.5 MW cited from [24]. The controllable parameters in this case are the power generation by generators at bus 61, bus 65, bus 66, bus 87, bus 89 and bus 100.

Fig. 6 plots the probability density function of P_{W59} and P_{W80} affected by wind speed. The shape and scale parameters of wind speed are set as $\alpha = 2$ and $\beta = 12$, while the cut-in, cut-out and rated wind speed for WTs are $v_{ci} = 3$ m/s, $v_{ct} = 25$ m/s and $v_{rd} = 12$ m/s [24], respectively. According to as Eq. (9), the output of wind farms is determined by the random parameter wind speed v_w, so it is also a random variable as shown in this figure.

Fig. 7 plots the probability density function of active power flow in lines L118-76, L98-80, L75-70 and L81-68 obtained by the SCM and MCM respectively, the shaded part in light blue is the operating range that satisfy the stability constraint. As can be seen from this figure, apart from line L98-80, the active power flow of lines has a certain probability to run outside the stable range affected by the randomness of wind speed. To quantitatively evaluate the approximation error of the proposed SCM, we use the following maximum percentage error $\delta_{y.\max}(\mathbf{p})$ as the error index:

$$\delta_{y.\max}(\mathbf{p}) \triangleq \text{Max}\{|y(\mathbf{p}) - \hat{y}(\mathbf{p})|/y(\mathbf{p})\}, \tag{24}$$

where Max{·} stands for the maximum computation, $y(\mathbf{p})$ is the actual value of y with parameter $\mathbf{p}$, $\hat{y}(\mathbf{p})$ is the approximated value.

The approximation error and computation time of SCM with $N-th$ order of polynomial bases and the MCM with 10000 samplings is shown in Table 3. As we can see, though the computation time increases with N for the SCM, the computation time using Monte Carlo method is much more than the SCM. Like the results in the 3-machine 9-bus system case, the results in table 3 show that the approximation error becomes smaller as the order of the polynomial basis function increases. The approximation error of the proposed method is very small in the whole range of uncertain parameters as the maximum percentage error does not exceed 5.7% in this case when the order of polynomial approximation is 3, which shows the effectiveness of the proposed method for approximating the statistical characteristic of static states.

In order to verify the effectiveness of the proposed method in solving the SOPF problem, Table 4 compares the control

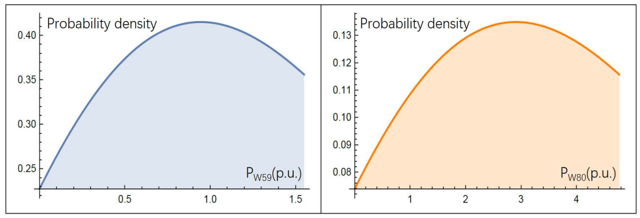

FIGURE 6. Probability density function of P_{W59} and P_{W80}.

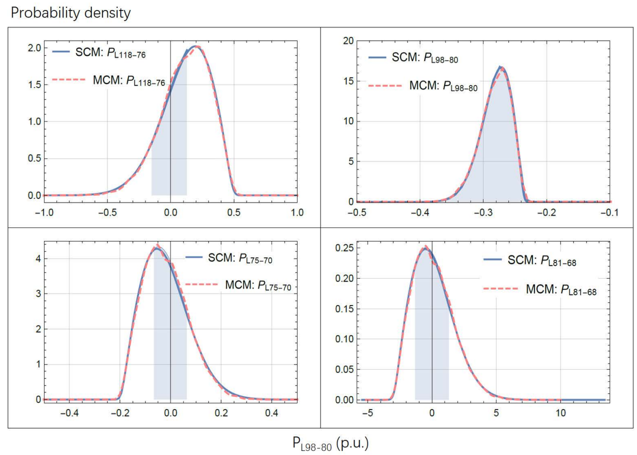

FIGURE 7. Probability density function of $P_{L118-76}$, P_{L98-80}, P_{L75-70} and P_{L81-68} obtained by the SCM and MCM.

TABLE 3. Computation time and error of the polynomial approximation of static states based on the SCM in IEEE 118-bus system case.

Method	$\delta_{PL1.\max}$	$\delta_{PL2.\max}$	$\delta_{PL3.\max}$	$\delta_{PL4.\max}$	Total time
MCM	–	–	–	–	24250s
SCM(1)	7.552%	5.842%	5.899%	5.974%	12.125s
SCM(2)	5.444%	4.738%	5.848%	5.298%	31.156s
SCM(3)	5.328%	4.576%	5.700%	5.105%	69.703s

effect of the control schemes obtained by the proposed method and by solving the OPF with rated output of wind farms. The OPF is implemented with uncertain parameters $P_{W59} = 154.5$ MW, $P_{W80} = 477$ MW. From Table 4 we can see that the fuel cost of the control scheme obtained by the proposed SOPF is higher than that of the control scheme obtained by the OPF. The reason is that the SOPF considers the security constraints of the power system, and the dispatchable generating units in need to change the power flow by changing their output, which leads to a relatively high fuel cost. In addition to this, the number of times the line power flow satisfy their constraints is different when different methods are used. Because there is no constraint on the line power flow in the OPF, the number of times the line power flow L118-76, L75-70, and L81-68 satisfy their limits in 1000 power flow calculations are 616, 705, and 844 respectively, and the out-of-limit probability is 38.4% in this case. For the SOPF, the number of times the

TABLE 4. Optimization results of the OPF and the proposed SOPF in IEEE 118-bus system case.

Method	Cost	N_1[1]	N_2[1]	N_3[1]	N_4[1]	$Pr\%$[2]	Total time
OPF	429.532	616	1000	705	844	38.4%	64.219s
SOPF	467.781	925	1000	923	975	7.7%	4.563s

[1] N is the number of times the line power flow $P_{\text{L118-76}}$, $P_{\text{L98-80}}$, $P_{\text{L75-70}}$, $P_{\text{L81-68}}$ satisfy their limits in 1000 power flow calculations
[2] $Pr\%$ is the out-of-limit probability of the optimal control scheme

line power flow L118-76, L75-70, and L81-68 satisfy their limits in 1000 power flow calculations are 925, 923, and 975 respectively, so the out-of-limit probability is only 7.7% when using this method, which is much smaller than that of the OPF. Therefore, even though the fuel cost of the proposed SOPF is slightly higher than that of the OPF, it can ensure that the operating state of the system meets the safety constraint. It is worth noting that for line L98-80, the line power flow always satisfies the constraint no matter which method is used, which is consistent with the results in Fig. 7. That is to say, the power flow of the line is guaranteed to be within its limits regardless of the variation of the wind farm's output.

VI. CONCLUSION

In this paper, a SCOPF problem is investigated for power system preventive control so as to enhance the static stability security affected by uncertain wind power generation. The solution of the SOPF problem is obtained using polynomial approximation based on the stochastic collocation method (SCM), which reformulates the probabilistic SOPF model into a deterministic one by explicitly depicts the relationship between the probability of chance constraint satisfication and uncertain parameters. Tests and analysis on the modified 3-machine 9-bus system and the IEEE 118-bus system have demonstrated the validity of the SOPF model for improving the probabilistic security level and the effectiveness of the SCM. Compared with the widely used MCM, the proposed SCM-based method has higher computation efficiency while the solution quality is generally comparable.

REFERENCES

[1] J. A. Momoh, R. J. Koessler, M. S. Bond, B. Stott, D. Sun, A. Papalexopoulos, and P. Ristanovic, "Challenges to optimal power flow," *IEEE Trans. Power Syst.*, vol. 12, no. 1, pp. 444–455, Feb. 1997.
[2] D. Gan, R. J. Thomas, and R. D. Zimmerman, "Stability-constrained optimal power flow," *IEEE Trans. Power Syst.*, vol. 15, no. 2, pp. 535–540, May 2000.
[3] H. Wei, H. Sasaki, J. Kubokawa, and R. Yokoyama, "An interior point nonlinear programming for optimal power flow problems with a novel data structure," *IEEE Trans. Power Syst.*, vol. 13, no. 3, pp. 870–877, Aug. 1998.
[4] K. Xie, Y. H. Song, J. Stonham, E. Yu, and G. Liu, "Decomposition model and interior point methods for optimal spot pricing of electricity in deregulation environments," *IEEE Trans. Power Syst.*, vol. 15, no. 1, pp. 39–50, Feb. 2000.
[5] Y.-C. Wu, A. S. Debs, and R. E. Marsten, "A direct nonlinear predictor-corrector primal-dual interior point algorithm for optimal power flows," *IEEE Trans. Power Syst.*, vol. 9, no. 2, pp. 876–883, May 1994.
[6] W.-M. Lin, S.-J. Chen, and Y.-S. Su, "An application of interior-point based OPF for system expansion with FACTS devices in a deregulated environment," in *Proc. PowerCon. Int. Conf. Power Syst. Technol.*, Dec. 2000, pp. 1407–1412.
[7] J. Cao, W. Du, and H. F. Wang, "Weather-based optimal power flow with wind farms integration," *IEEE Trans. Power Syst.*, vol. 31, no. 4, pp. 3073–3081, Jul. 2016.
[8] X. Dui, G. Zhu, and L. Yao, "Two-stage optimization of battery energy storage capacity to decrease wind power curtailment in grid-connected wind farms," *IEEE Trans. Power Syst.*, vol. 33, no. 3, pp. 3296–3305, May 2018.
[9] C. Peng, P. Xie, L. Pan, and R. Yu, "Flexible robust optimization dispatch for hybrid wind/photovoltaic/hydro/thermal power system," *IEEE Trans. Smart Grid*, vol. 7, no. 2, pp. 751–762, Mar. 2016.
[10] Y. Xu, J. Ma, Z. Y. Dong, and D. J. Hill, "Robust transient stability-constrained optimal power flow with uncertain dynamic loads," *IEEE Trans. Smart Grid*, vol. 8, no. 4, pp. 1911–1921, Jul. 2017.
[11] A. Lorca and X. Sun, "Adaptive robust optimization with dynamic uncertainty sets for multi-period economic dispatch under significant wind," *IEEE Trans. Power Syst.*, vol. 30, no. 4, pp. 1702–1713, Jul. 2015.
[12] W. Wu, J. Chen, B. Zhang, and H. Sun, "A robust wind power optimization method for look-ahead power dispatch," *IEEE Trans. Sustain. Energy*, vol. 5, no. 2, pp. 507–515, Apr. 2014.
[13] R. A. Jabr, "Adjustable robust OPF with renewable energy sources," *IEEE Trans. Power Syst.*, vol. 28, no. 4, pp. 4742–4751, Nov. 2013.
[14] M. Madrigal, K. Ponnambalam, and V. H. Quintana, "Probabilistic optimal power flow," in *Proc. IEEE Can. Conf. Electr. Comput. Eng.*, May 1998, pp. 385–388 vol. 1.
[15] A. Schellenberg, W. Rosehart, and J. Aguado, "Cumulant based probabilistic optimal power flow (P-OPF)," in *Proc. Int. Conf. Probabilistic Methods Appl. Power Syst.*, Sep. 2004, pp. 506–511.
[16] A. Schellenberg, W. Rosehart, and J. Aguado, "Cumulant-based probabilistic optimal power flow (P-OPF) with Gaussian and gamma distributions," *IEEE Trans. Power Syst.*, vol. 20, no. 2, pp. 773–781, May 2005.
[17] A. Schellenberg, W. Rosehart, and J. Aguado, "Introduction to cumulant-based probabilistic optimal power flow (P-OPF)," *IEEE Trans. Power Syst.*, vol. 20, no. 2, pp. 1184–1186, May 2005, doi: 10.1109/TPWRS.2005.846188.
[18] G. Verbic and C. A. Canizares, "Probabilistic optimal power flow in electricity markets based on a two-point estimate method," *IEEE Trans. Power Syst.*, vol. 21, no. 4, pp. 1883–1893, Nov. 2006.
[19] Z. Q. Xie, T. Y. Ji, M. S. Li, and Q. H. Wu, "Quasi-Monte Carlo based probabilistic optimal power flow considering the correlation of wind speeds using copula function," *IEEE Trans. Power Syst.*, vol. 33, no. 2, pp. 2239–2247, Mar. 2018.
[20] J. Wang, M. Shahidehpour, and Z. Li, "Security-constrained unit commitment with volatile wind power generation," *IEEE Trans. Power Syst.*, vol. 23, no. 3, pp. 1319–1327, Aug. 2008.
[21] L. Wu, M. Shahidehpour, and T. Li, "Stochastic security-constrained unit commitment," *IEEE Trans. Power Syst.*, vol. 22, no. 2, pp. 800–811, May 2007.
[22] Q. Wang, Y. Guan, and J. Wang, "A chance-constrained two-stage stochastic program for unit commitment with uncertain wind power output," *IEEE Trans. Power Syst.*, vol. 27, no. 1, pp. 206–215, Feb. 2012.
[23] A. Papavasiliou, S. Oren, and R. O'Neill, "Reserve requirements for wind Power integration: A scenario-based stochastic programming framework," *IEEE Trans. Power Syst.*, vol. 26, no. 4, pp. 2197–2206, Nov. 2011.
[24] S. Xia, X. Luo, K. W. Chan, M. Zhou, and G. Li, "Probabilistic transient stability constrained optimal power flow for power systems with multiple correlated uncertain wind generations," *IEEE Trans. Sustain. Energy*, vol. 7, no. 3, pp. 1133–1144, Jul. 2016.
[25] M. Hajian, W. D. Rosehart, and H. Zareipour, "Probabilistic power flow by Monte Carlo simulation with Latin supercube sampling," *IEEE Trans. Power Syst.*, vol. 28, no. 2, pp. 1550–1559, May 2013.
[26] D. Shen, H. Wu, B. Xia, and D. Gan, "Polynomial chaos expansion for parametric problems in engineering systems: A review," *IEEE Syst. J.*, vol. 14, no. 3, pp. 4500–4514, Sep. 2020.
[27] D. Xiu, *Numerical Methods for Stochastic Computations: A Spectral Method Approach*. Princeton, NJ, USA: Princeton Univ. Press, 2010.
[28] J. R. Hockenberry and B. C. Lesieutre, "Evaluation of uncertainty in dynamic simulations of power system models: The probabilistic collocation method," *IEEE Trans. Power Syst.*, vol. 19, no. 3, pp. 1483–1491, Aug. 2004.

[29] B. Xia, H. Wu, Y. Qiu, B. Lou, and Y. Song, "A Galerkin method-based polynomial approximation for parametric problems in power system transient analysis," *IEEE Trans. Power Syst.*, vol. 34, no. 2, pp. 1620–1629, Mar. 2019.
[30] Y. Zhou, H. Wu, C. Gu, and Y. Song, "A novel method of polynomial approximation for parametric problems in power systems," *IEEE Trans. Power Syst.*, vol. 32, no. 4, pp. 3298–3307, Jul. 2017.
[31] Y. Qiu, J. Lin, F. Liu, and Y. Song, "Explicit MPC based on the Galerkin method for AGC considering volatile generations," *IEEE Trans. Power Syst.*, vol. 35, no. 1, pp. 462–473, Jan. 2020.
[32] A. Kaintura, T. Dhaene, and D. Spina, "Review of polynomial chaos-based methods for uncertainty quantification in modern integrated circuits," *Electronics*, vol. 7, no. 3, p. 30, Feb. 2018.
[33] H. N. Najm, "Uncertainty quantification and polynomial chaos techniques in computational fluid dynamics," *Annu. Rev. Fluid Mech.*, vol. 41, no. 1, pp. 35–52, Jan. 2009.
[34] K.-K. K. Kim, D. E. Shen, Z. K. Nagy, and R. D. Braatz, "Wiener's polynomial chaos for the analysis and control of nonlinear dynamical systems with probabilistic uncertainties [historical perspectives]," *IEEE Control Syst. Mag.*, vol. 33, no. 5, pp. 58–67, 2013.
[35] I. Pena, C. B. Martinez-Anido, and B.-M. Hodge, "An extended IEEE 118-bus test system with high renewable penetration," *IEEE Trans. Power Syst.*, vol. 33, no. 1, pp. 281–289, Jan. 2018.

BINGQING XIA was born in Hunan, China, in 1994. She received the Ph.D. degree in electrical engineering from Zhejiang University. She is currently with Powerchina Huadong Engineering Corporation Ltd. Her current research interests include power system transient analysis and reactive power management.

YUWEI CHEN received the Ph.D. degree in electrical engineering from Zhejiang University, Hangzhou, China, in 2021. Since 2021, she has been working as a Postdoctoral Researcher with Powerchina Huadong Engineering Corporation Ltd., Hangzhou, co-cultured by the College of Electrical Engineering, Zhejiang University. Her current research interests include model and optimization algorithms of non-linear systems.

WENBIN YANG, photograph and biography not available at the time of publication.

QING CHEN, photograph and biography not available at the time of publication.

XIAOHE WANG, photograph and biography not available at the time of publication.

KUAN MIN, photograph and biography not available at the time of publication.